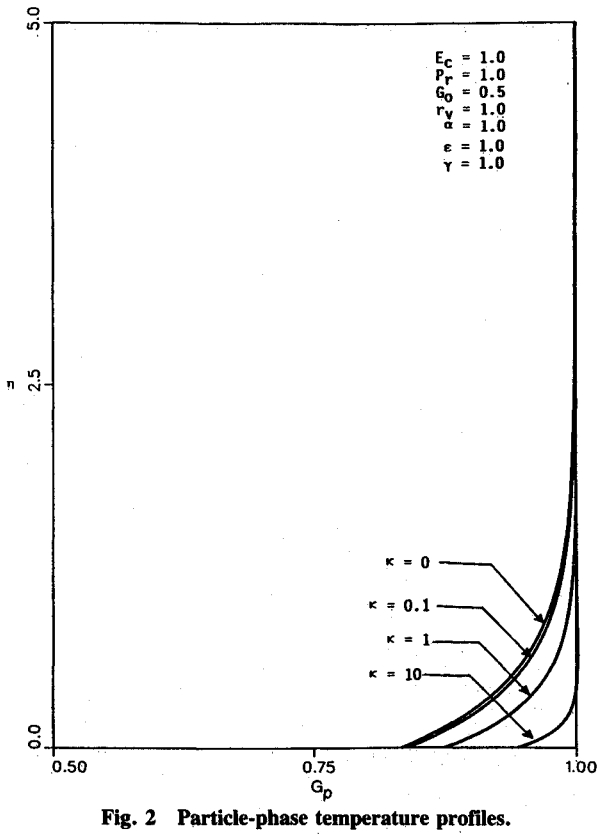

Fig. 2 Particle-phase temperature profiles.

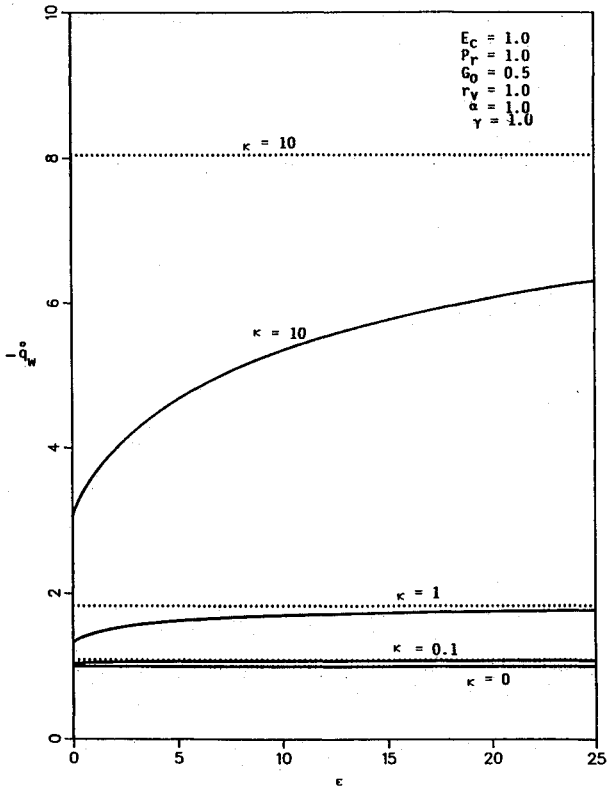

Fig. 3 Wall heat transfer coefficient vs ε.

less than unity, the temperature of the freestream. This is evident from Fig. 3. The fact that the fluid and particle phase temperatures exceed the freestream temperature for large values of κ is probably due to the work caused by drag between the two phases (last term in Eq. (3b)), which is not present for single-phase flow.

Figure 3 illustrates the influence of the particle loading κ and the temperature inverse Stokes number ε on the wall heat transfer coefficient $\dot{q}_w$. The dotted lines indicate the limits approached as $\varepsilon \to \infty$ (thermal equilibrium limit). Increases in the particle loading κ cause G to approach the freestream temperature faster; thus, increasing the fluid-phase temperature gradient at the wall. This is reflected in the increases in $\dot{q}_w$ caused by increasing κ. Increases in the temperature inverse Stokes number ε cause an increase in the thermal interaction between the two phases. This increases the interphase energy transfer between the two phases, and, therefore, increases the fluid-phase temperature at any position above the plate. This steepening effect produces the same results discussed above; namely, an increase in the wall heat transfer coefficient.

Conclusion

Exact solutions for the thermal aspect of flow of a particulate suspension past an infinite porous flat plate were obtained. Numerical computations of the exact solutions were performed and the computed results were presented graphically to illustrate the properties of this type of flow. It was concluded that the presence of particles causes an augmentation in the wall heat transfer coefficient. This is due to the thermal energy gain by the fluid phase through the thermal interaction between the two phases.

References

[1]Soo, S. L., "Boundary Layer Motion of a Gas-Solid Suspension," University of Illinois, Project Squid Report ILL-3P, 1961.

[2]Marble, F. E., "Dynamics of Dusty Gases," *Annual Review of Fluid Mechanics*, Vol. 2, 1970, pp. 297–446.

[3]Schlichting, H., Boundary Layer Theory, Pergamon, New York, 1955, p. 230–232.

[4]Chamkha, A. J., and Peddieson, J., "Exact Solutions of the Two-Phase Asymptotic Suction Profile," *Developments in Theoretical and Applied Mechanics*, Vol. 14, 1988, pp. 215–222.

Transient Combined Conduction and Radiation in Anisotropically Scattering Spherical Media

Hsin-Sen Chu* and Ling-Chia Weng†
National Chiao Tung University,
Hsinchu, Taiwan, 30049 Republic of China

Introduction

IN the design of many engineering systems, radiative heat transfer can be an important mode of heat transfer. Much research has been conducted on the analysis of simultaneous radiation and conduction in absorbing, emitting, and scattering one-dimensional planeparallel systems.[1,2] The analysis of radiative transfer in spherical media has been the subject of relatively few investigations, although there are important applications in numerous areas, such as spherical propulsion systems, nuclear energy generation and explosions, astrophysics, and thermal insulation systems.

Many of the previous investigations on radiative transfer in spherically symmetric geometry have been limited to the special case of an absorbing, emitting medium.[3,4] There are

Received May 24, 1991; revision received Aug. 16, 1991; accepted for publication Aug. 16, 1991.

*Professor, Department of Mechanical Engineering.
†Graduate Student, Department of Mechanical Engineering.

several works that have included the effects of scattering by suspended particles within the medium.[5-9] It seems that there are no studies considering the transient combined conduction and radiation in an anisotropically scattering medium between two concentric sphere, although there are important applications of such problem.

The present work is concerned with transient interaction of conduction and radiation in an absorbing, emitting, and anisotropically scattering concentric spherical medium. The major difficulty in the analysis of such a problem stems from the nonlinear integral-differential character of thermal radiative transfer. The present study utilizes the spherical harmonics method. A time-marching, fully implicit algorithm is employed to solve the energy equation. Emphases are given the effect of scattering phase function and optical radius on transient radiative and total heat flux distributions during interaction between conduction and radiation in the medium.

Formulation

Consider an absorbing, emitting, and anisotropically scattering, concentric, spherical medium that is initially at a uniform temperature T_0. At time $t > 0$, the inner and outer boundary surfaces are subjected to a constant temperature T_1 and T_2, respectively. Both diffuse and specular reflections at boundaries are included. Under these conditions, the dimensionless transient energy equation can be expressed as

$$\frac{\partial\theta(R,\xi)}{\partial\xi} = \frac{\partial^2\theta(R,\xi)}{\partial R^2} + \frac{2}{R}\frac{\partial\theta(R,\xi)}{\partial R} - \frac{\tau_2}{NR^2}\frac{\partial(R^2Q^r)}{\partial R} \quad (1)$$

associated with the following initial and boundary conditions:

$$\theta(R_1,\xi) = 1,\ \theta(1,\xi) = \theta_2,\ \theta(R,0) = \theta_0 \quad (2)$$

where we have introduced the following dimensionless quantities:

$$N = \frac{k_c\sigma_e}{4\sigma T_1^3},\ \xi = \frac{k_c t}{\rho c_p r_2^2},\ Q^r = \frac{q^r}{4\sigma T_1^4},\ I = \frac{i}{4\sigma T_1^4},\ R = \frac{r}{r_2} \quad (3)$$

and $\tau_2 = \sigma_e r_2$ is the optical radii distance in outer spheres, ω is the single scattering albedo, and $\theta = T/T_1$. The dimensionless intensity I satisfies the radiative transfer equation

$$\mu\frac{\partial I(R,\mu)}{\partial R} + \frac{1-\mu^2}{R}\frac{\partial I(R,\mu)}{\partial\mu} + \tau_2 I(R,\mu) = \frac{(1-\omega)\tau_2\theta^4}{4\pi} + \frac{\omega\tau_2}{2}\int_{-1}^{1} P(\mu,\mu')\, I(R,\mu')\, d\mu',\quad R_1 < R < 1 \quad (4)$$

with the boundary conditions

$$I(R_1,\mu) = \frac{\varepsilon_1}{4\pi} + \rho_1^s I(R_1,-\mu) + 2\rho_1^d\int_0^1 I(R_1,-\mu')\,\mu'\,d\mu',\quad \mu > 0 \quad (5)$$

$$I(1,-\mu) = \frac{\varepsilon_2\theta_2^4}{4\pi} + \rho_2^s I(1,\mu) + 2\rho_2^d\int_0^1 I(1,\mu')\,\mu'\,d\mu',\quad \mu > 0 \quad (6)$$

where ε is the emissivity, ρ^s and ρ^d are the specular and diffuse reflectivities, respectively. The assumption that $\varepsilon + \rho^s + \rho^d = 1$ has been used.[9]

Method of Solution

Because of the complexity of the radiation nature as well as the nonlinear dependency of radiation emission on temperature, analytic solutions are difficult to obtain. The following solutions are obtained with the radiation contribution solved by P_N method and the energy equation solved by time-marching, fully implicit algorithm.

In the spherical harmonics and method for the solution of the radiative transfer equation in the medium, the scattering phase function $P(\mu,\mu')$ and radiant intensity $I(R,\mu)$ can be expanded in a series of Legender polynomials, Eq. (4) is reduced to the following system of ordinary differential equation (ODE):

$$(m+1)\frac{d\Psi_{m+1}(R)}{dR} + m\frac{d\Psi_{m-1}(R)}{dR} + (m+1)(m+2)\frac{\Psi_{m+1}(R)}{R} - m(m-1)\frac{\Psi_{m-1}(R)}{R} + \tau_2(2m+1)(1-\omega a_m)\Psi_m(R) - \tau_2(1-\omega)\theta^4\delta_{0m} = 0,\quad m = 0,1,2,\ldots,N \quad (7)$$

where the values of a_m are dependent upon the type of scattering being modeled. To be compatible with the spherical harmonic approximation, the boundary conditions must be reformulated using Marshak's boundary conditions, which require the moments of the radiant intensity to be conserved instead of the intensity itself. Therefore, Eqs. (5-6) become

$$\int_0^1 I(R_1,\mu)\mu^{2\ell-1}\,d\mu = \int_0^1\left[\frac{\varepsilon_1}{4\pi} + \rho_1^s I(R_1,-\mu) + 2\rho_1^d\int_0^1 I(R_1,-\mu')\mu'\,d\mu'\right]\mu^{2\ell-1}\,d\mu,\quad \mu > 0 \quad (8)$$

$$\int_0^1 I(1,-\mu)\mu^{2\ell-1}\,d\mu = \int_0^1\left[\frac{\varepsilon_2\theta_2^4}{4\pi} + \rho_2^s I(1,\mu) + 2\rho_2^d\int_0^1 I(1,\mu')\mu'\,d\mu'\right]\mu^{2\ell-1}\,d\mu,\quad \mu > 0 \quad (9)$$

where $\ell = 1, 2, 3, \ldots, (2N+1)/2$.

For the P_N approximation, the series of Eq. (7) is truncated at N, resulting in $N+1$ ordinary differential equations. High-order approximations have been discussed by Bayazitoglu and Higenyi,[10] and the third-order approximation is shown to be quite accurate for spherical media. The P_3 approximation is addressed in the following section.

In the P_3 approximation, four ODEs result from Eq. (7), which are

$$\frac{d\Psi_1}{dR} + 2\frac{\Psi_1}{R} + \tau_2(1-\omega)\Psi_0 - \tau_2(1-\omega)\theta^4 = 0 \quad (10)$$

$$2\frac{d\Psi_2}{dR} + \frac{d\Psi_0}{dR} + 6\frac{\Psi_2}{R} + 3\tau_2(1-\omega a_1)\Psi_1 = 0 \quad (11)$$

$$3\frac{d\Psi_3}{dR} + 2\frac{\Psi_1}{dR} + 12\frac{\Psi_3}{R} + 5\tau_2\Psi_2 = 0 \quad (12)$$

$$3\frac{d\Psi_2}{dR} - 6\frac{\Psi_2}{R} + 7\tau_2\Psi_3 = 0 \quad (13)$$

where, by definition, $\Psi_0(R)$ and $\Psi_1(R)$ are the incident radiation and the radiant heat flux, respectively. In the field of heat transfer, it is usually these two quantities that are of

interest, rather than the intensity itself. Thus, only the solutions for $\Psi_0(R)$ and $\Psi_1(R)$ are presented. After differencing the unsteady term $\partial\theta/\partial\xi$ using three-term backward differences, Eq. (1) becomes

$$\frac{d^2\theta^\ell}{dR^2} = \frac{1.5\theta^\ell - 2\theta^{\ell-1} + 0.5\theta^{\ell-2}}{\Delta\xi} - \frac{2}{R}\frac{d\theta^\ell}{dR} + \frac{\tau_2^2(1-\omega)}{NR^2}(\theta^{\ell,4} - \Psi_0) \tag{14}$$

where $\Delta\xi$ is the dimensionless time-step, and ℓ, $\ell - 1$, and $\ell - 2$ are the present, the last, and the one before the last times, respectively. The partial differential equation is transformed into an ODE for a given time-step. Equations (10–14) constitute a system of four first ODE equation in $\Psi_i (i = 0, 1, 2,$ and 3) and a second-order ODE in θ. The four boundary conditions for Ψ_i are supplied by Eqs. (8–9) and two boundary conditions for θ are specified in Eq. (2). After separating the second-order ODE into two first order ODEs, the resulting system of six first-order ODEs are solved by using BVPFD from a commercial software IMSL. Once the temperature and radiative heat flux are known, the total heat flux in the medium is given by

$$Q^t(R, \xi) = \frac{q^t r_2}{k_c T_1} = -\frac{\partial\theta(R\,\xi)}{\partial R} + \frac{\tau_2 Q^r}{N} \tag{15}$$

The marching procedure is continued until the steady state is assured. In present study, the steady state is defined as the state where

$$|Q_j^{r,\ell} \times R_j^2 - Q_1^{r,\ell} \times R_1^2| < 1 \times 10^{-4} \tag{16}$$

was met at all mesh points. The results were obtained by carrying out the numerical algorithm on a VAX 8800 at National Chiao Tung University.

Results and Discussion

Although the present fully implicit, time-marching, finite difference technique is unconditionally stable, there are time-step constraints to yield physically realistic solutions. A numerical experiment is carried out here to ensure the independence of numerical results on the time-step $\Delta\xi$. The time-step is determined to be 0.00025 for all cases. To illustrate the accuracy of the numerical solution of present work, results of steady nondimensional heat transfer are compared with that of Viskanta and Merriam[5] for the isotropic scattering case. Table 1 shows the comparisons at $\theta_2 = 0.5$, $R_1 = 0.5$, $\omega = 0$, $\varepsilon_1 = \varepsilon_2 = 1$, and $N = 0.1$ for several optical radii. It is shown that the comparisons are in excellent agreement. Figure 1 shows the variation of total heat flux with respect to dimensionless time at three positions at $\theta_2 = 0$, $\tau_1 = 2$, $\tau_2 = 4$, $\varepsilon_1 = \varepsilon_2 = 1$, $\omega = 0.5$, and $N = 0.01$. It is shown that more time is required for a strongly back-scattering system to reach steady state than a strongly forward-scattering one.

Table 1 Comparison of the steady heat flux with isotropic scattering on the boundary at $\theta_2 = 0.5$, $R_1 = 0.5$, $\omega = 0$, $\varepsilon_1 = \varepsilon_2 = 1.0$, and $N = 0.1$ for several optical radii

	Inner wall			Outer wall		
τ_2	Q^c	Q^r	Q^t	Q^c	Q^r	Q^t
2	2.559[a]	0.183[a]	6.244[a]	0.724[a]	0.040[a]	1.519[a]
	2.485[b]	0.188[b]	6.250[b]	0.745[b]	0.040[b]	1.562[b]
4	3.005[a]	0.138[a]	8.511[a]	1.056[a]	0.027[a]	2.128[a]
	2.965[b]	0.141[b]	8.630[b]	1.063[b]	0.027[b]	2.157[b]
10	3.470[a]	0.080[a]	11.455[a]	1.562[a]	0.013[a]	2.864[a]
	3.482[b]	0.080[b]	11.506[b]	1.572[b]	0.013[b]	2.876[b]

[a]Visktanta and Merriam.[5]
[b]Present results.

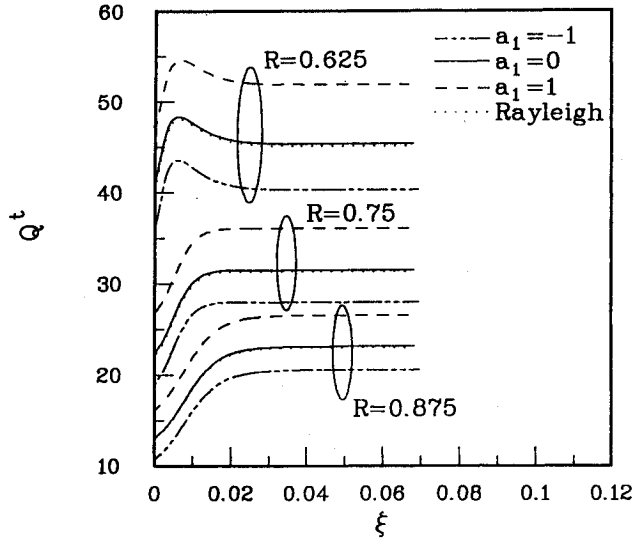

Fig. 1 Variation of heat flux with respect to time at three positions for $\theta_0 = \theta_2 = 0$, $\varepsilon_1 = \varepsilon_2 = 1$, $\omega = 0.8$, $\tau_1 = 2$, $\tau_2 = 4$, and $N = 0.01$.

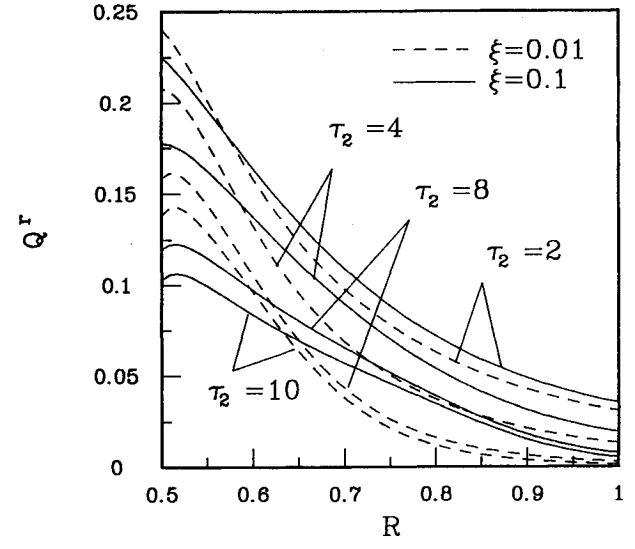

Fig. 2 The effect of optical radius on the radiative heat flux at $\theta_0 = \theta_2 = 0$, $\varepsilon_1 = \varepsilon_2 = 1$, $\omega = 0.5$, $R_1 = 0.5$, and $N = 0.01$.

This is because radiant energy emitted by the medium is transferred more easily to the boundaries if the medium is forward scattering rather than backward scattering. However, the difference between the isotropic and Rayleigh scattering is small. Figure 2 shows the effect of optical radii on the radiative heat flux at $\theta_2 = 0$, $\varepsilon_1 = \varepsilon_2 = 1$, $\omega = 0.5$, $R_1 = 0.5$, and $N = 0.01$ for isotropic scattering. It reveals that the maximum value of radiative heat flux has a peak value near the hot wall for large values of τ_2 due to the effects of absorption and emission. Based on the results of this study, it is also found that at large values of optical radii the radiative flux decreases and the interaction between the two modes of heat transfer leads to an increase in the conductive flux, as shown in Table 1. The reason for this is that for fixed geometry, an increase in optical radii corresponds to an increase in the absorption coefficient, thereby increasing the emission of energy from hot medium near the hot wall.

Conclusion

An analysis of the transient energy transfer due to the combined effects conduction and radiation for anisotropically scattering between two concentric spheres has been analyzed. The P_3 method is utilized to solve the radiative transfer, while a time-marching algorithm is proposed to deal the unsteady

energy equation. It is shown in present numerical analysis that the phase function and optical radii have significant effect on heat flux distribution of the problem considered.

Acknowledgments

This research was supported by the National Science Council of the Republic of China through Grants NSC 79-0401-E009-14.

References

[1]Tong, T. W., McElroy, D. L., and Yarbrough, D. W., "Transient Conduction and Radiation Heat Transfer in Porous Thermal Insulation," *Journal of Thermal Insulation,* Vol. 9, July 1985, pp. 13–29.

[2]Barker, C., and Sutton, W. H., "The Transient Radiation and Conduction Heat Transfer in a Gray Participating Medium with Semi-Transparent Boundaries," *ASME Radiation Heat Transfer,* edited by B. F. Armaly and A. F. Emery, HTD-Vol. 49, 1985, pp. 25–36.

[3]Sparrow, E. M., Usiskin, C. M., and Huibbard, H. A., "Radiation Heat Transfer in a Spherical Enclosure Contained in Participating, Heat-Generation Gas," *Journal of Heat Transfer,* Vol. 83, No. 2, 1961, pp. 199–206.

[4]Ryhming, I. L., "Radiative Transfer Between Two Concentric Spheres Separated by an Absorbing and Emitting Gas," *International Journal of Heat and Mass Transfer,* Vol. 9, April 1966, pp. 315–324.

[5]Viskanta, R., and Merriam, R. L., "Heat Transfer by Combined Conduction and Radiation Between Concentric Spheres Separated by Radiation Medium," *Journal of Heat Transfer,* Vol. 90, May 1968, pp. 248–256.

[6]Thynell, S. T., and Özisik, M. N., "Radiation Transfer in an Isotropically Scattering Homogeneous Solid Sphere," *Journal of Quantitative Spectroscopy and Radiative Transfer,* Vol. 33, No. 4, 1985, pp. 383–395.

[7]Thynell, S. T., "Interaction of Conduction and Radiation in Anisotropically Scattering Spherical Media," *Journal of Thermophysics and Heat Transfer,* Vol. 4, No. 3, 1990, pp. 299–304.

[8]Tong, T. W., and Swathi, P. S., "Radiative Heat Transfer in Emitting-Absorbing-Scattering Spherical Medium," *Journal of Thermophysics and Heat Transfer,* Vol. 1, No. 2, 1987, pp. 162–170.

[9]Li, W., and Tong, T. W., "Radiative Heat Transfer in Isothermal Spherical Media," *Journal of Quantitative Spectroscopy and Radiative Transfer,* Vol. 43, No. 3, 1990, pp. 239–251.

[10]Bayazitoglu, Y., and Higenyi, J., "Higher-Order Differential Equations of Radiative Transfer: P_3 Approximation," *AIAA Journal,* Vol. 17, No. 4, 1979, pp. 424–431.

Backward Monte Carlo Modeling for Rocket Plume Base Heating

H. F. Nelson*
University of Missouri—Rolla, Rolla, Missouri 65401

Introduction

RADIATIVE base heating of a rocket due to its exhaust plume has been investigated actively for several years. Reviews of the analysis of base heating prior to 1966 are available.[1,2] Methods for making practical calculations have been developed.[3–6]

Radiation emitted from a participating medium with a conical geometry is difficult to analyze compared to slab, or cylindrical geometries. Gorshkova[7] used a zonal method to solve for the radiation in a truncated cone with isotropic scattering and constant properties. Kaminski[8] used both a Monte Carlo and a P-1 approximation to investigate radiative heat transfer from a nonscattering medium with uniform properties in a truncated cone enclosure. Lin and Wang[9] calculated the radiation from an absorbing, isotropic scattering, conical medium. They investigated the influence of cone angle and cone length on the radiation heating of the exterior base region. Their geometry was similar to that for the plume radiation heating of the base of a rocket.

Studies of plume radiation have been performed for conical geometries. Bobco[10,11] and Edwards[12] developed a plume model to predict base heating. The radiation was described in terms of radiosity that varied axially along the plume. Edwards and Bobco[13] and Edwards et al.[14] also formulated an engineering model to predict the radiosity of conical plumes. Watson and Lee[15] used a Monte Carlo model to calculate the radiation from solid rocket plumes. The model accounted for axial and radial property variations of both the particles and the gases in the plume. The scattering was allowed to be either isotropic or anisotropic.

The purpose of this note is 1) to show that the backward Monte Carlo method can be used to predict radiative heating for geometries similar to those for rocket plume base heating, and 2) to compare the backward Monte Carlo predictions with previous work done by other methods. The motivation for this research is to develop a computer code to calculate the base heating of a rocket due to its plume radiation. The backward Monte Carlo model seems to be the best way to calculate the radiative base heating from realistic plumes.

Formulation

Figure 1 shows a schematic of the rocket plume and base heating geometry. The origin of the coordinate system is at the center of the rocket nozzle exit plane. The base of the rocket is located at $z = -z_0$, where z_0 is the length of the rocket nozzle. The radiation flux from a point $\boldsymbol{x}_p$ on the plume to a point $\boldsymbol{x}_0$ on the base is defined as

$$F_\lambda(\boldsymbol{x}_0) = \int_{\Delta\Omega} \varepsilon_\lambda(\boldsymbol{x}_p, \theta', \phi') I_{b\lambda}(T_{\text{ref}}) \cos\theta \, d\Omega \qquad (1)$$

where, $\varepsilon_\lambda(\boldsymbol{x}_p, \theta', \phi')$ is the radiation emission coefficient, θ is the angle between the vector $\boldsymbol{n}_r$, along the line connecting points $\boldsymbol{x}_0$ and $\boldsymbol{x}_p$ and the outward normal vector $\boldsymbol{n}_0$ at $\boldsymbol{x}_0$ on the rocket base, $\Delta\Omega$ is the solid angle of the plume as viewed from the point $\boldsymbol{x}_0$ and θ' and ϕ' represent the polar and azimuthal angular orientation of the radiation intensity ray with respect to an outward normal vector $\boldsymbol{n}_p$ at point $\boldsymbol{x}_p$. The reference Planck intensity is $I_{b\lambda}(T_{\text{ref}})$, where T_{ref} is the reference temperature (normally the maximum temperature in the plume). Note that the medium between points $\boldsymbol{x}_0$ and $\boldsymbol{x}_p$ is noninteracting. In the Monte Carlo analysis it is assumed that the photon does not lose any energy as it travels from its point of emission in the plume, to the plume boundary; hence, the emission at $\boldsymbol{x}_p$ is directly related to the temperature

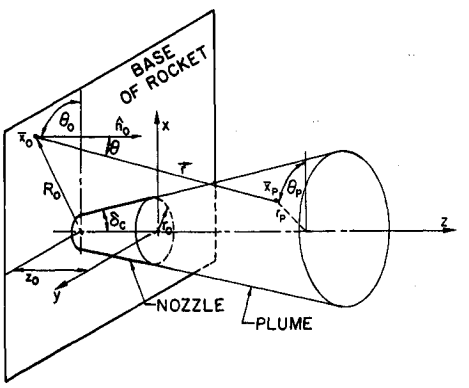

Fig. 1 Schematic of the rocket plume geometry.

Received June 5, 1991; revision received Aug. 26, 1991; accepted for publication Aug. 26, 1991.

* Professor of Aerospace Engineering, Thermal Radiative Transfer Group, Department of Mechanical and Aerospace Engineering and Engineering Mechanics. Associate Fellow AIAA.